Supplementary information

One-Pot Ligation-PCR for Universal RNA Biomarker Detection

Jinding Liu,[a†] Zhixin Xie,[a†] Nini Li,[a] Jiajia Li,[a] Minghua Zhang,[b*] Yongqiang Cheng,[a*] and Jiangyan Zhang[a*]

[a] Key Laboratory of Medicinal Chemistry and Molecular Diagnosis (Hebei University), Ministry of Education, Key Laboratory of Analytical Science and Technology of Hebei Province, College of Chemistry and Materials Science, Hebei University, Baoding, 071002, Hebei, P. R. China.

[b] Affiliated Hospital of Hebei University, Baoding, 071002, Hebei, P. R. China.

*Corresponding Authors: zhangmhhbdxfy@163.com (M. Zhang),

yqcheng@hbu.edu.cn (Y. Cheng), zhangjiangyan@hbu.edu.cn (J. Zhang).

†These authors contributed equally to this work.

Table of Contents

1. The sequences of the nucleic acids used in this assay

Table S1. The sequences of the nucleic acids used in this assay

Name	Sequences (5′-3′ direction)
BRCA1-Δ (9,10)	AAAAGACGUCUGUCUACAUUGAAUUGGCUGCUUGUGAAUUUUCUGAGACG
BRCA1-Δ (11q,3642-)	UGAGAGGCAUCCAGAAAAGUAUCAGGGUGAAGCAGCAUCUGGGUGUGAG
BRCA1-Δ (11q,333-)	AGAGCAAAGCAUGGAUUCAAACUUAGGUGAAGCAGCAUCUGGGUGUGAG
miR-21	UAGCUUAUCAGACUGAUGUUGA
Δ (9,10)- probe A	PO_4-CAATTCAATGTAGACAGACGTCTTGTACCGCTCTATGGGCAGTCGGTGAT
Δ (9,10)- probe B	CCATCTCATCCCTGCGTGTCTCAGTTGTCTCAGAAAATTCACAAGCAGC
Δ (11q,3642-)-probe A	PO_4-CCTGATACTTTTCTGGATGCCTCCTCTATGGGCAGTCGGTGAT
Δ (11q,3642-)-probe B	CCATCTCATCCCTGCGTGTCACACCCAGATGCTGCTTCAC
Δ (11q,333-)-probe A	PO_4-CTAAGTTTGAATCCATGCTTTGCTACTCTATGGGCAGTCGGTGAT
Δ (11q,333-)-probe B	CCATCTCATCCCTGCGTGTCACACCCAGATGCTGCTTCAC
miR-21-probe A	PO_4-CTGATAAGCTAAAGTCGGTCGCCTCTATGGGCAGTCGGTGAT
miR-21-probe B	CCATCTCATCCCTGCGTGTCACTACCTTCACTCAACATCAGT
Forprimer	ATCACCGACTGCCCATAGAG
Revprimer	CCATCTCATCCCTGCGTGTC

2. Electrophoresis analysis of primers

Primers were chemically caged with glyoxal and analyzed by electrophoresis. As shown in Fig. S1, glyoxal-caged primers (lanes 2 and 5) migrated more slowly than untreated primers (lanes 1 and 4), confirming successful modification. Upon thermal treatment, the migration of decaged primers (lanes 3 and 6) returned to the same position as the untreated primers, demonstrating that the glyoxal adducts could be efficiently removed by heating. These results verify that glyoxal modification is reversible and thermally controllable, fulfilling the requirement for sequential reaction activation in a one-pot format.

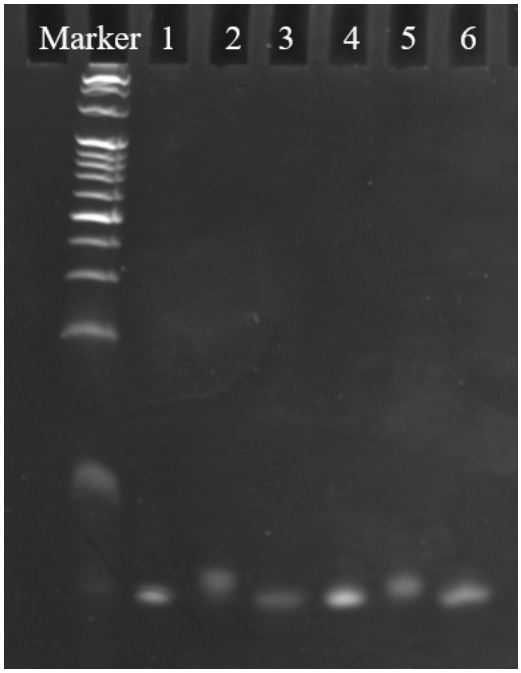

Fig. S1 20% denaturation PAGE assay of untreated, caged and decaged primer. To decage the primer, 2 μM of caged primer (1 h glyoxal treatment time) was incubated at 95 °C and pH 7.5 for 40 min. The primers were stained with GelRed following 20% denaturing PAGE. Lane 1 is the untreated Forprimer (2 μM), Lane 2 is the caged Forprimer (5 μM), Lane 3 is the decaged Forprimer (2 μM), Lane 4 is the untreated Revprimer (2 μM), Lane 5 is the caged Revprimer (5 μM), Lane 6 is the decaged Revprimer (2 μM)

3. Two-step ligation-PCR using both untreated primers and glyoxal-caged primers

We first conducted a two-step PCR using untreated primers and glyoxal-caged primers to evaluate the compatibility of glyoxal-caged primers with PCR amplification. As shown in Fig. S2a, using untreated primers, the fluorescence amplification curves exhibit a leftward shift, with earlier cycle threshold (C_T) values as the concentration increases, enabling detection down to as low as 1 fM. Similarly, with glyoxal-caged primers (Fig. S2b), the fluorescence amplification curves also shift leftward as concentration increases, reaching a detection of 1 fM. For the same target concentration, higher C_T values were observed when glyoxal-caged primers were used. In addition, the baseline of amplification curves obtained with glyoxal-caged primers displayed a gradual upward trend during the early PCR cycles (except for baseline fluctuations within the first approximately five cycles), rather than remaining flat. This is consistent with that the glyoxal-caged primers are not fully released during the initial high-temperature incubation, followed by gradual decaging during the early PCR cycles. Such gradual primer release may contribute to the observed baseline increase. Importantly, both untreated and glyoxal-caged primers enabled reliable detection at the femtomolar level, confirming that glyoxal modification is compatible with PCR amplification.

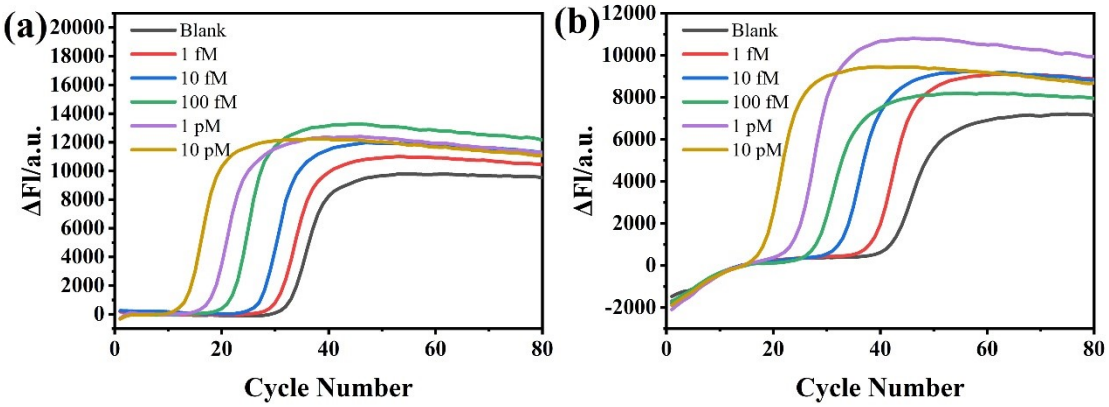

Fig. S2 Fluorescence amplification curves of two-step ligation-PCR using both untreated primers (a) and glyoxal-caged primers (b). The target is BRCA1-Δ (9,10), and the concentration refers to the concentration in a final volume of 10 μL.

4. Effect of residual glyoxal concentration on PCR amplification

To evaluate whether residual glyoxal released during thermal decaging could affect PCR amplification performance, control experiments were conducted using a conventional two-step PCR workflow, in which glyoxal was directly added to the PCR reaction mixture at defined concentrations. This design isolates the effect of free glyoxal on PCR amplification from the ligation step and allows assessment of potential interference with DNA polymerase activity or fluorescence readout.

The forward primer sequence was ATCACCGACTGCCCATAGAG, which contains four guanine residues, and the reverse primer sequence was CCATCTCATCCCTGCGTGTC, which contains three guanine residues. In the PCR reaction, each primer was used at a final concentration of 0.2 μM. Based on the total guanine content of the primer pair, a reference glyoxal concentration of 1.4 μM was calculated. This concentration represents a near-stoichiometric reference level relative to the total guanine content of the primers and does not imply complete or site-specific modification. In addition to this reference level, higher glyoxal concentrations (14 μM and 140 μM) were tested to probe potential effects under excess glyoxal conditions.

PCR amplification was performed under otherwise identical conditions, and amplification curves and C_T values were compared across different glyoxal concentrations. As shown in Fig. S3, no systematic shift in C_T

values or abnormal amplification behavior was observed across the tested glyoxal concentration range. Although minor variations in fluorescence intensity were occasionally observed, these variations did not translate into significant differences in amplification thresholds.

These results indicate that residual glyoxal, even at concentrations exceeding those relevant to the one-pot ligation-PCR system, does not substantially inhibit PCR amplification or compromise quantitative readout under the conditions tested.

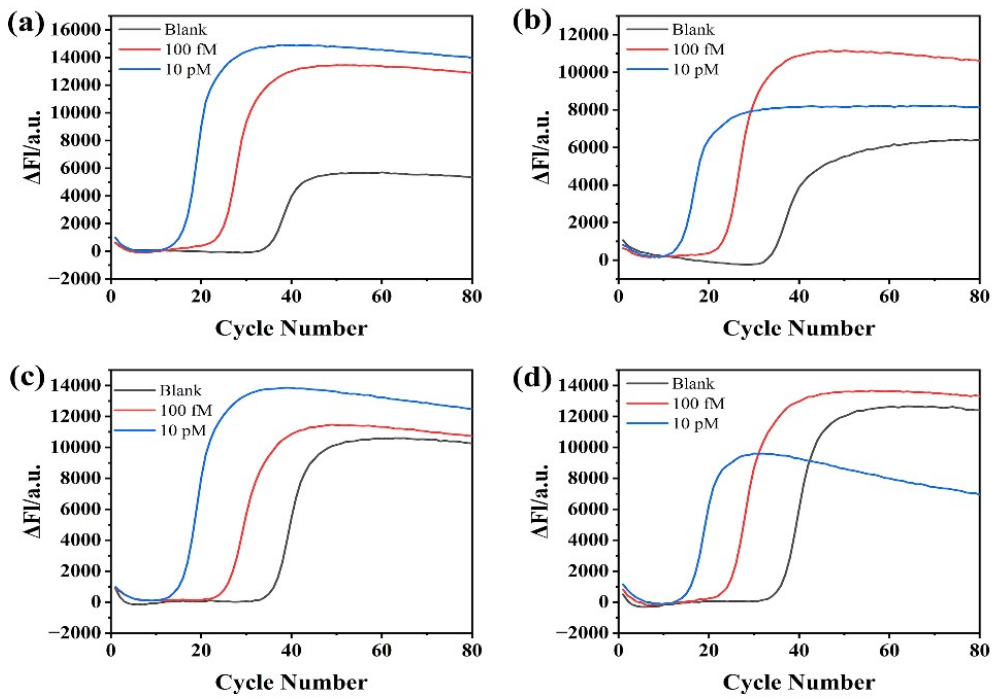

Fig. S3 Effect of residual glyoxal concentration on PCR amplification performance in a two-step PCR assay. Real-time fluorescence amplification curves obtained in the presence of different glyoxal concentrations: (a) 0 μM glyoxal, (b) 1.4 μM glyoxal, (c) 14 μM glyoxal, and (d) 140 μM glyoxal. The target BRCA1-Δ (9,10) were 0, 100 fM, and 10 pM, respectively.

5. Optimization of the amount of Ex Taq HS DNA polymerase reaction buffer

To establish appropriate reaction conditions for the one-pot ligation-PCR system, the amount of Ex Taq HS DNA polymerase reaction buffer was optimized. Buffer concentrations of 0.1×, 0.25×, 0.5×, and 1× were evaluated using 10 pM and 1 pM RNA targets, together with blank controls to assess background amplification, as shown in Fig. S4. At a buffer concentration of 0.1×, no amplification curves were observed in either the sample or blank groups, indicating that the polymerase activity was too low at this dosage to support normal PCR amplification. As the buffer concentration increased, distinct amplification curves appeared for both the sample and blank groups, with C_T values gradually decreasing. At a buffer concentration of 0.25×, the C_T values for the 10 pM and 1 pM samples showed a significant difference, with the most pronounced separation between the C_T values of the 1 pM sample and the blank controls.

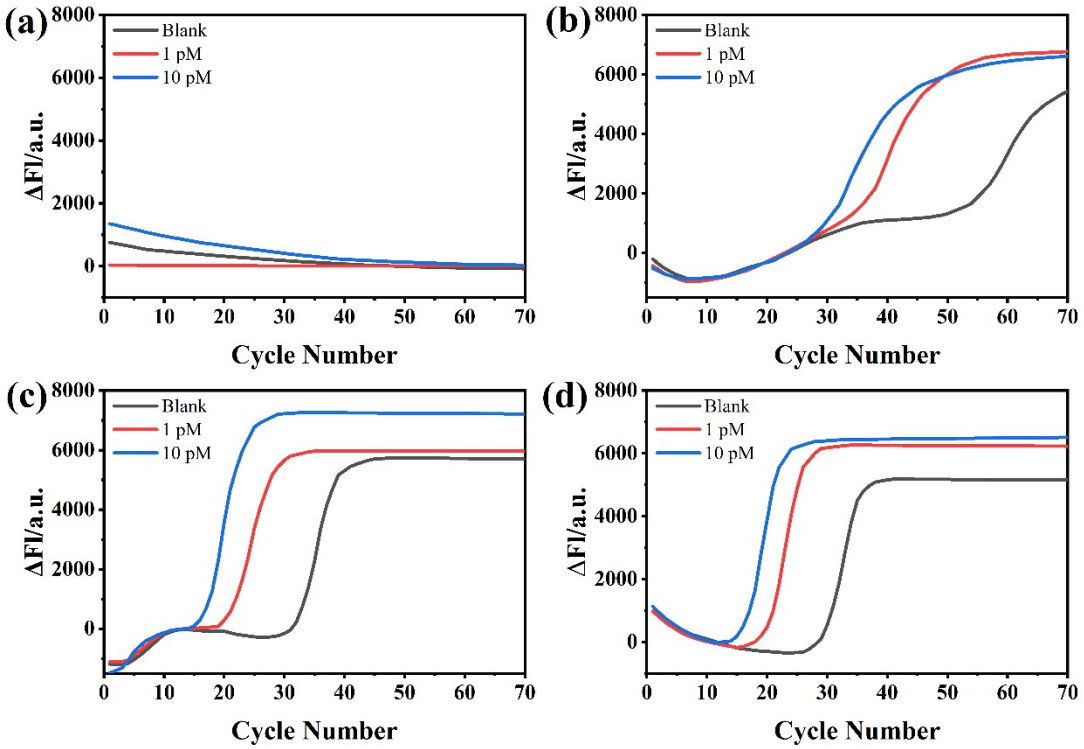

Fig. S4 Effect of the Ex Taq buffer concentration on the ligation-PCR assay. The Ex Taq HS DNA Polymerase buffer concentration was 0.1×(a), 0.25×(b), 0.5×(c), and 1×(d).

6. Optimization of the amount of SplintR ligase reaction buffer

The buffer composition within the assay system plays a critical role in modulating enzyme activity and therefore requires careful optimization. As shown in Fig. S5, when the concentration of SplintR ligase reaction buffer was increased from 0.05× to 0.5×, the C_T values of both the sample and blank groups gradually decreased, indicating enhanced overall reaction efficiency. At low buffer concentrations, reduced ligation efficiency was observed, which subsequently affected downstream PCR amplification. Although the exact contribution of individual buffer components was not systematically examined, these results clearly demonstrate that the concentration of SplintR ligase reaction buffer has a pronounced impact on assay performance. When the SplintR ligase reaction buffer concentration was set to 0.1×, the difference in C_T values between the blank and the 1 pM sample was maximized, providing the clearest discrimination. Therefore, 0.1× was selected as the optimal concentration of SplintR ligase reaction buffer for the one-pot ligation-PCR detection system.

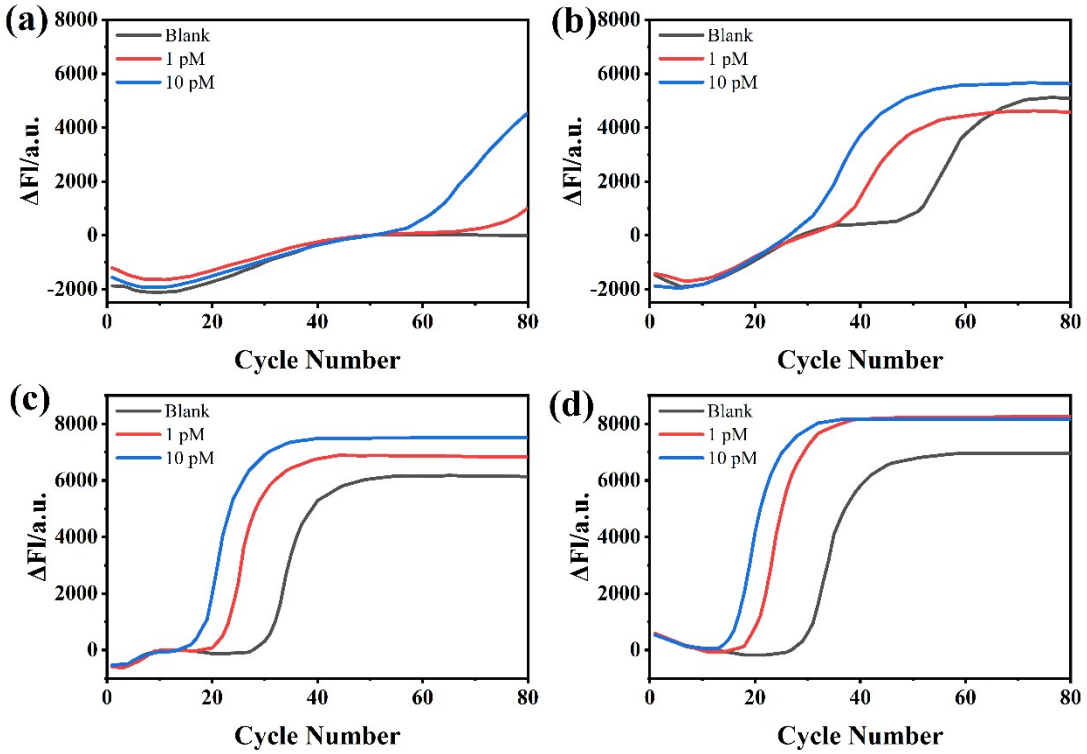

Fig. S5 Effect of the SplintR ligase reaction buffer concentration on the ligation-PCR assay. The SplintR ligase reaction buffer concentration was 0.05×(a), 0.1×(b), 0. 25×(c), and 0.5×(d).

7. Optimization of the amount of SplintR ligase

Monovalent cations inhibit the activity of SplintR ligase. To maintain the stability of SplintR ligase during storage, NEB uses a storage buffer containing 300 mM NaCl. The company strongly recommends that the concentration of these common reactants (NaCl, KCl) in the reaction remains below 50 mM. For optimizing the dosage of SplintR ligase, we tested four different units (1.25 U, 2.5 U, 3.75 U) to detect 10 pM and 1 pM mRNA samples, as well as blank amplification curves, as shown in Fig. S6. When the amount of SplintR ligase was set at 2.5 U, we observed an optimal distinction between the C_T values of 1 pM and 10 pM samples, with the greatest difference between the C_T values of the 1 pM sample and the blank. Consequently, we selected 2.5 U of SplintR ligase as the optimal concentration for the one-pot ligaiton-PCR detection system.

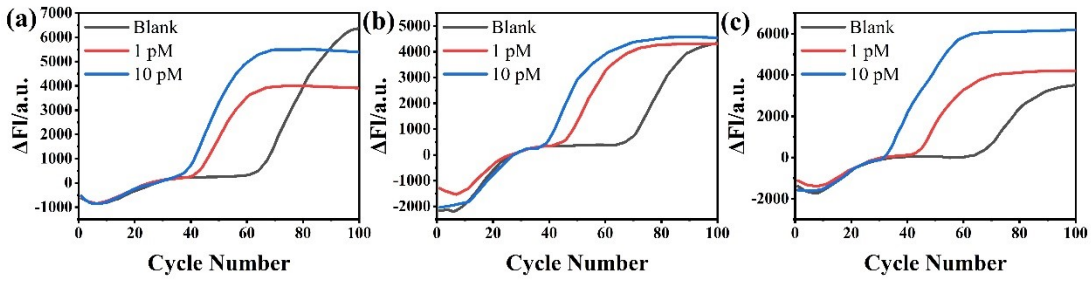

Fig. S6 Effect of the SplintR ligase amount on the ligation-PCR assay. The amount of SplintR ligase was 1.25 U (a), 2.5 U (b), 3.75 U (c).

8. Optimization of the amount of Ex Taq HS DNA polymerase

Ex Taq HS DNA polymerase is a formulation of anti-Taq monoclonal antibodies and TaKaRa Ex Taq DNA polymerase, designed to prevent non-specific amplification caused by unintended primer annealing or primer dimer formation at lower temperature. This polymerase is well-suited for Hot Start PCR. The enzyme dosage is a critical factor influencing amplification efficiency. We tested various dosages of Ex Taq HS DNA polymerase at 0.25 U, 0.5 U, and 0.75 U to determine the optimal conditions, assessing the amplification of 10 pM and 1 pM mRNA samples, as well as blank controls. At a dosage of 0.25 U, both the sample and blank groups showed high C_T values, as illustrated in Fig. S7, with minimal distinction between the 1 pM sample and the blank, indicating insufficient enzyme concentration and low PCR efficiency. Increasing the dosage to 0.5 U resulted in a significant decrease in C_T values for the sample group, leading to a clearer separation from the blank group. However, further increases to 0.75 U caused a rise in the C_T value of the blank group, likely due to non-specific elongation from excess enzyme activity. Consequently, we selected 0.5 U of Ex Taq HS DNA polymerase as the optimal concentration for the one-pot detection system.

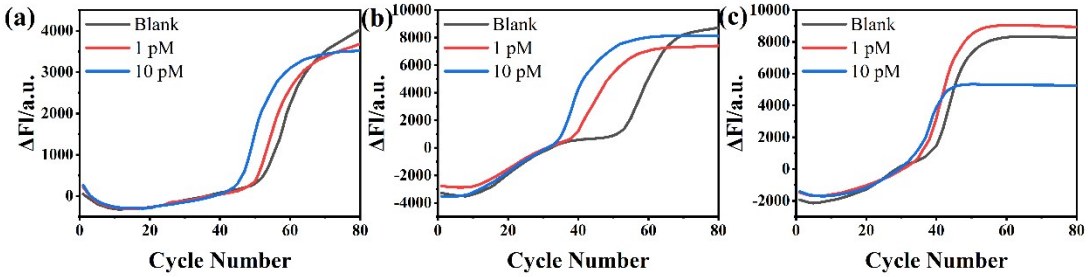

Fig. S7 Effect of the Ex Taq HS DNA polymerase amount on the ligation-PCR assay. The amount of Ex Taq HS DNA polymerase was 0.25 U (a), 0.5 U (b), 0.75 U (c), and 1 U (d).

9. Optimization of the amount of glyoxal-caged primers

The concentration of glyoxal-caged primers plays a critical role in influencing the amplification efficiency of the PCR reaction. As shown in Fig. S8, at a primer concentration of 50 nM, neither the sample nor the blank control exhibited any amplification curve, suggesting that this concentration was insufficient for effective PCR amplification. With increasing primer concentrations, amplification curves became evident. Additionally, as the primer concentration increased, the amplification curves for both the sample and the blank control shifted forward, indicating enhanced amplification efficiency. However, at a concentration of 400 nM, the blank control exhibited a more pronounced shift, likely due to elevated non-specific amplification at higher primer concentrations. At a primer concentration of 200 nM, the distinction between the sample and the blank was most pronounced. Thus, a primer concentration of 200 nM was chosen as the optimal condition for the one-pot detection system.

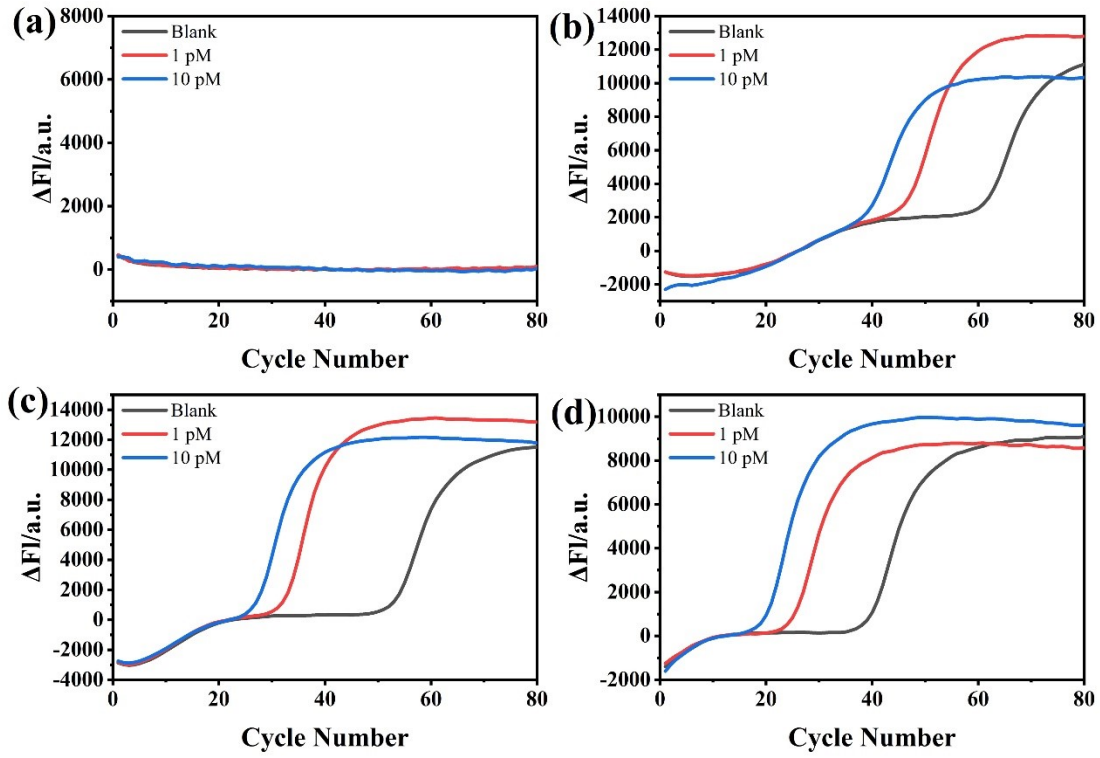

Fig. S8 Effect of the primer concentration on the ligation-PCR assay. The primer concentration was 50 nM (a), 100 nM (b), 200 nM (c), and 400 nM (d).

10. Batch-to-batch reproducibility of glyoxal-caged primers

To evaluate batch-to-batch reproducibility of the glyoxal modification process, glyoxal-caged primers were independently prepared in three separate modification reactions conducted on different days, while all subsequent ligation-PCR experiments were performed using the same reagent set and enzyme preparation.

As shown in Fig. S9, the three independently modified primer batches exhibited comparable amplification behavior, including consistent target–blank separation and similar amplification trends across concentrations. Although minor differences in absolute C_T values were observed, such variation is commonly observed in qPCR-based assays and does not affect relative quantification, particularly when standard curves are freshly generated for each experimental run. Importantly, the overall assay performance and discrimination capability were preserved across all batches.

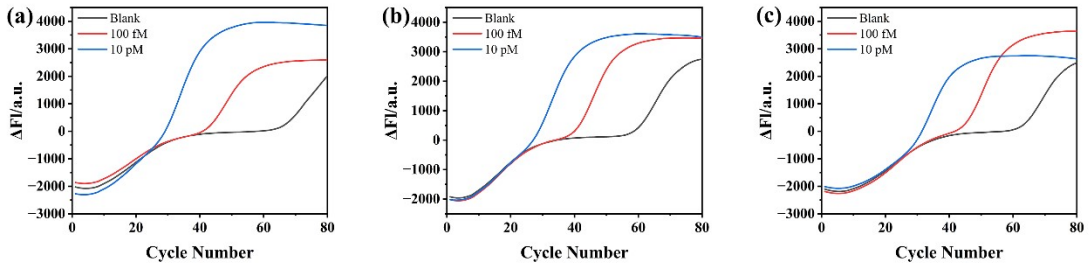

Fig. S9 Batch-to-batch reproducibility of glyoxal-caged primers prepared in three independent modification reactions. Panels (a–c) show real-time fluorescence amplification curves obtained using primers modified on different days. Blank, 100 fM, and 10 pM RNA target.

11. Storage stability of glyoxal-caged primers

To specifically evaluate the storage stability of glyoxal-caged primers, a separate batch of primers was prepared following glyoxal modification and ethanol precipitation. In contrast to the primers used in routine experiments, which were dissolved and stored in solution, the glyoxal-caged primers for the stability study were kept in the precipitated state without redissolution and stored at −20 °C.

After storage for 0, 3, 6, 9, 12, and 15 days, aliquots of the precipitated primers were freshly redissolved in RNase-free water immediately before use and subjected to real-time ligation-PCR analysis under identical conditions. As shown in Fig. S10, highly consistent amplification profiles were obtained across all storage times, with clear and reproducible separation between blank samples and target concentrations (100 fM and 10 pM).

Importantly, no noticeable increase in background amplification or loss of target discrimination was observed with prolonged storage, indicating that glyoxal caging remains chemically stable during storage in the precipitated state. These results demonstrate that glyoxal-caged primers exhibit excellent storage stability for at least 15 days without compromising assay specificity or quantitative performance.

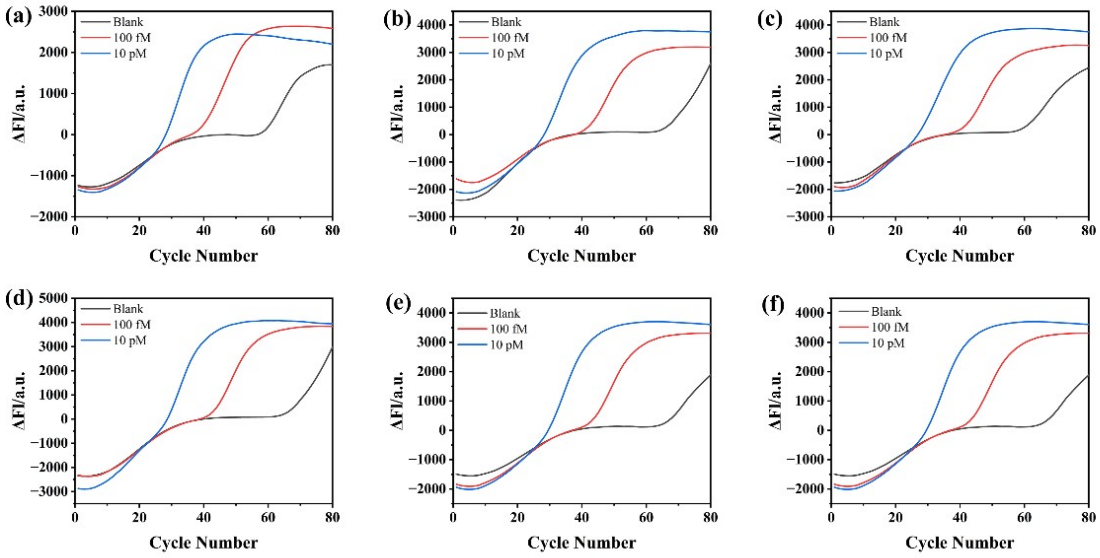

Fig. S10 Storage stability of glyoxal-caged primers stored in the precipitated state. Real-time fluorescence amplification curves obtained using glyoxal-caged primers stored as ethanol precipitates at −20 °C for (a) 0, (b) 3, (c) 6, (d) 9, (e) 12, and (f) 15 days. Blank, 100 fM, and 10 pM RNA targets were analyzed after freshly redissolving the primers prior to the ligation-PCR assay.

12. Specificity evaluation for BRCA1 splice variants

Table S2. Relative detection of BRCA1 splice variants using different probe sets.

Target splice variant	Δ(9,10) probe	Δ(11q,3642−) probe	Δ(11q,333−) probe
Δ(9,10)	**100%**	≤ 0.024%	≤ 0.027%
Δ(11q,3642−)	≤ 0.012%	**100%**	≤ 0.015%
Δ(11q,333−)	≤ 0.027%	≤ 0.023%	**100%**
Summed non-target interference	**≤ 0.039%**	**⩽ 0.047%**	**⩽ 0.042%**

Note: Relative detection values were calculated based on ΔCt analysis using the corresponding standard curves, with the signal of the cognate splice variant normalized to 100%. Relative signals from non-cognate variants were calculated individually and further summed to estimate the total non-target interference, following the reporting convention adopted in previous ligation-PCR studies. Values represent conservative upper-bound estimates obtained from three independent replicates (n = 3).

13. Amplification profiles and quantitative performance of the two-step ligation-PCR assay

As shown in Fig. S11, the two-step ligation-PCR assay produced typical sigmoidal amplification curves for the target RNA over a wide concentration range, with earlier amplification observed at higher target concentrations and a clear separation from the blank control. Based on the amplification data, a calibration curve was constructed by plotting the C_T values against the logarithm of the target concentration. A good linear relationship was obtained over the tested concentration range, described by the equation $C_T = -5.567 \log C - 48.38$, with a correlation coefficient of $R^2 = 0.9950$. These results indicate that the two-step ligation-PCR method provides reliable quantitative performance and serves as a suitable reference for evaluating the analytical characteristics of the one-pot ligation-PCR strategy.

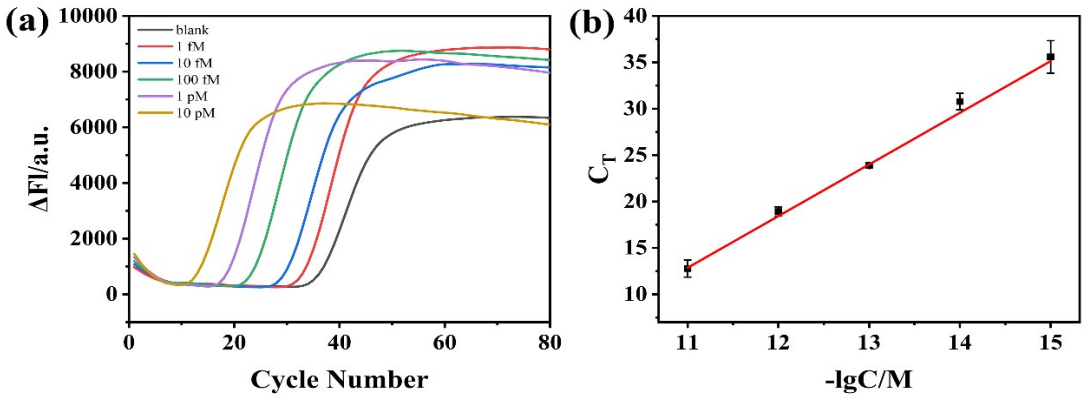

Fig. S11 Amplification profiles and quantitative performance of the two-step ligation-PCR assay. (a) Real-time fluorescence amplification curves obtained for the target RNA at different concentrations (1 fM–10 pM), together with the blank control. (b) Linear relationship between the C_T values and the logarithm of the target concentration derived from the amplification data, demonstrating the quantitative performance of the two-step ligation-PCR method. Error bars represent the standard deviation of three independent measurements (n = 3).

14. Specificity evaluation of the glyoxal-assisted one-pot ligation-PCR assay for miR-21 detection

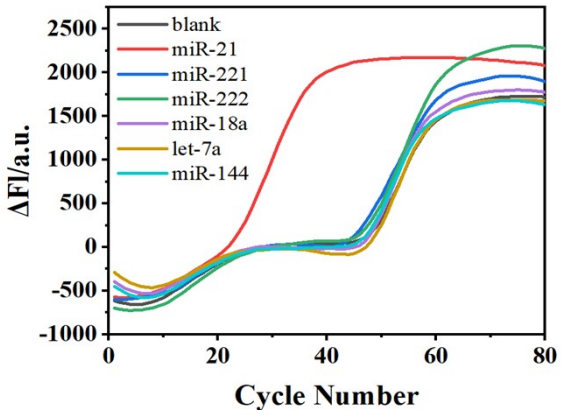

Fig. S12 Real-time amplification curves for miR-21 and non-related microRNAs (each at 100 pM) obtained using the glyoxal-assisted one-pot ligation-PCR assay.